Neocarzinostatin-Induced Hydrogen Atom Abstraction from C-4′ and C-5′ of the T Residue at a d(GT) Step in Oligonucleotides: Shuttling between Deoxyribose Attack Sites Based on Isotope Selection Effects†

Lizzy S. Kappen and Irving H. Goldberg*
Department of Biological Chemistry and Molecular Pharmacology, Harvard Medical School, Boston, Massachusetts 02115
Bruce L. Frank, Leroy Worth, Jr., Donna F. Christner, and John W. Kozarich*
Department of Chemistry and Biochemistry and Center for Agricultural Biotechnology, University of Maryland, College Park, Maryland 20742
JoAnne Stubbe*
Department of Chemistry, Massachusetts Institute of Technology, Cambridge, Massachusetts 02139
Received September 24, 1990; Revised Manuscript Received November 27, 1990

ABSTRACT: The thiol-activated neocarzinostatin chromophore cleaves duplex oligonucleotides containing the sequence -TGTTTGA-, producing 3′-phosphoglycolate and 3′-phosphate fragments at T, indicating the involvement of 4′- as well as 5′-chemistry at this residue. Substitution of deuterium for hydrogen at the C-4′ position of the affected T leads to a kinetic isotope effect (k_H/k_D) of 4.0 on the formation of the glycolate-ended product, whereas deuterium at C-5′ of the same T reveals k_H/k_D of 1.6 in the formation of the phosphate-ended product. The proportion of the products representing 4′- and 5′-chemistry can be shifted on the basis of isotope selection effects. A second product resulting from 4′-chemistry, the abasic site associated with 4′-hydroxylation, has been identified as an alkali-labile site, and as a pyridazine derivative formed after cleavage by hydrazine. A comparable isotope effect on its production (k_H/k_D = 3.7) relative to that of 3′-phosphoglycolate production is consistent with a common intermediate, a putative 4′-peroxy radical, in their formation. The formation of both products of 4′-chemistry is oxygen-dependent, and the internal partitioning between them (3′-phosphate or 3′-phosphoglycolate) is influenced by thiols. Moreover, the nitroaromatic radiation sensitizer misonidazole can substitute for dioxygen, yielding 3′-phosphoglycolate and alkali-labile 3′-phosphate ends, indicative of 4′-chemistry. In addition to the internal partitioning of 4′-chemistry, thiols also affect the overall extent of cleavage (4′ plus 5′) and the relative partitioning between both sites of attack (4′ or 5′).

The antitumor activity of the antibiotic neocarzinostatin (NCS)[1] is related to the ability of its nonprotein chromophore to induce damage in DNA [reviewed in Goldberg (1987)]. The proposed mechanism of DNA cleavage by the NCS chromophore is shown in Scheme I. Subsequent to activation by thiols (Scheme II), the NCS–thiol adduct collapses to form a putative biradical (NCS*) (Hensens et al., 1983; Edo et al., 1985; Myers, 1987; Goldberg, 1987; Myers et al., 1988) that can abstract a hydrogen from C-5′ of the deoxyribose moiety of thymidylate and adenylate residues (Scheme IA) (Kappen & Goldberg, 1985; Chin et al., 1988). The 5′-deoxyribose radical is trapped by O_2 to form peroxyl radical **1** that can in subsequent steps lead to a strand break containing predominantly nucleoside 5′-aldehyde (**4**) at the 5′-end and phosphate at the 3′-end (Kappen et al. 1982; Kappen & Goldberg, 1983). The major lesion has thus been established to involve C-5′ chemistry.

However, minor lesions, technically more difficult to investigate, may also be of biological significance. One example of a minor lesion is the mutagenically important, sequence-specific DNA cleavage at the C in d(AGC) sequences. This lesion involves NCS* attack at the C-1′ position of the deoxycytidylate residue and ultimately results in the release of cytosine and an abasic site containing a deoxyribonolactone moiety (Povirk & Goldberg, 1985a, 1986; Kappen et al., 1988, 1990; Kappen & Goldberg, 1989). A second example of a minor lesion reported by Saito et al. (1989) involves C-4′ chemistry (Scheme IB) at a T residue in a self-complementary hexamer d(CGTACG), producing thymine and a C-4′ hydroxylated abasic product (Scheme IB, **8**). The observation of C-4′ chemistry has recently been extended to a natural DNA, the *Hin*dIII–*Bam*HI 375 bp fragment of pBR322 containing [4′-^{2}H]- or [5′,5′-$^2H_2$]thymidine residues (Frank et al., 1990). Results from this study strongly suggested an internal partitioning, subject to isotopic discrimination, between 4′- and 5′-chemistry at d(GT) steps. In addition, not only was an abasic hydroxylated species produced and identified as a 3′-phosphate subsequent to alkaline treatment, but also a second species whose properties were consistent with a C-4′-derived phosphoglycolate moiety was produced (Scheme IB, **9**). The partitioning between these two moieties, as well as between C-4′ and C-5′ chemistry, appeared to be dependent on the thiol activator/reductant.

Quantitation and chemical identification of the products of minor lesions using large DNA substrates have proven to be analytically difficult. In order to more firmly identify the products produced by NCS during the C-4′ chemistry and to better quantitate the partitioning products of C-4′ attack as

† This work was supported by Grants CA 44257 and GM 12573 (I.H.G.) and GM 34454 (J.W.K. and J.S.) from the National Institutes of Health.

[1] Abbreviations: NCS, neocarzinostatin; NCS*, activated NCS; Glu, glutathione; MPA, 3-mercaptopropionate; BME, 2-mercaptoethanol; HTP, 4-hydroxythiophenol; BLM, bleomycin.

0006-2960/91/0430-2034$02.50/0

Scheme I

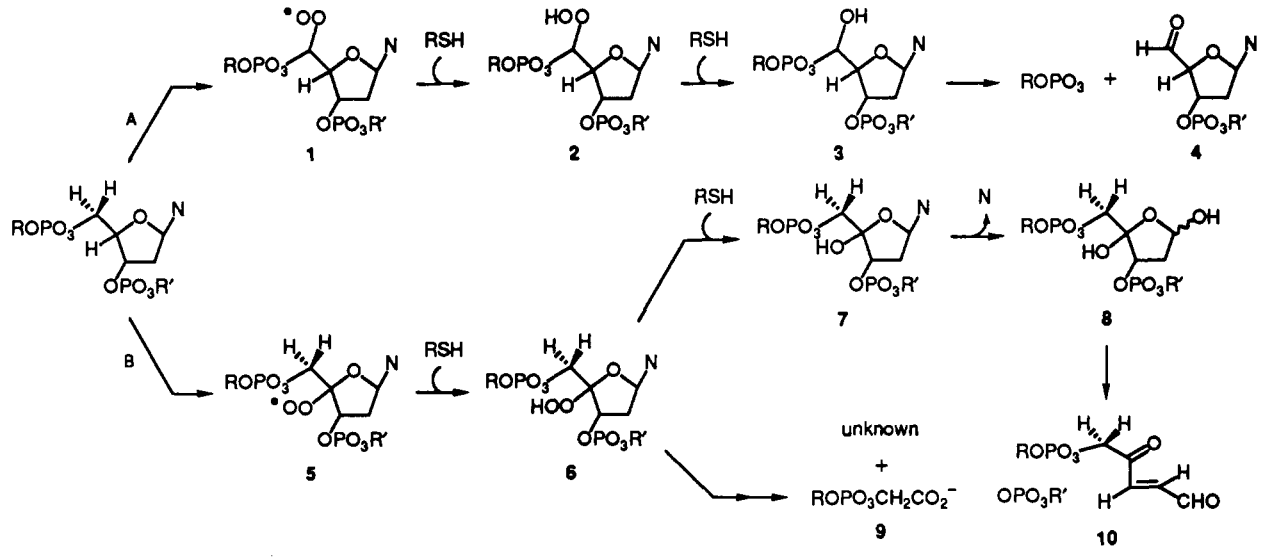

Scheme II

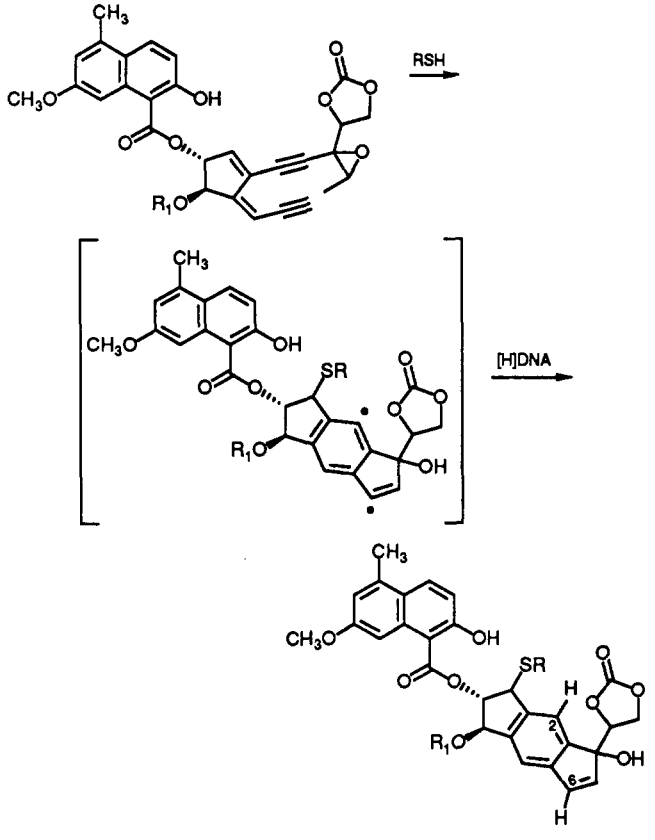

a function of thiol and ^2H substitution, two oligomers containing dGTT sequences, d(TTCTCATGTTTGA) and d(TGTTTGA), have now been studied in detail. Results reported herein establish unambiguously that (1) substitution of deuterium for hydrogen at the C-4′ or C-5′ positions of the first T residue causes a shift in the attack rate at each position due to isotopic discrimination; (2) the structure of the thiol (activator) utilized to generate NCS* directly affects the partitioning between 4′- and 5′-chemistry; (3) 3′-phosphoglycolate ends as well as alkali-labile abasic sites are generated as the major products of the 4′-chemistry; (4) the formation of these 4′-derived products is, in turn, affected by the structure of the thiol (reductant). Further, the production of both the 3′-phosphoglycolate and the 4′-hydroxylated abasic product is dependent on O_2, and under anaerobic conditions the radiation sensitizer misonidazole can substitute for O_2. A mechanistic hypothesis to account for the results at C-4′ is proposed. The implications of this mechanism with respect to C-4′ chemistry mediated by bleomycin are also discussed.

Materials and Methods

The materials and their sources are as follows: deoxyribonucleoside triphosphates, Pharmacia; [γ-^{32}P]ATP and [α-^{32}P]dATP (3000 Ci/mmol), New England Nuclear; misonidazole, Hoffmann-La Roche; Sep-Pak C-18 cartridges, Waters Associates; polynucleotide kinase and the Klenow fragment of DNA polymerase I, New England Biolabs; *Escherichia coli* endonuclease IV, a gift of Bruce Demple, Harvard University; Bleomycin, Bristol Laboratories; NCS, Kayaku Antibiotics. Deuterium-labeled thymidine triphosphates (5′-dideuterio and 4′-deuterio) were synthesized as described (Moss et al., 1963; Brown & Subba Rao, 1960; Ajmera et al., 1986a,b).

Preparation of Substrates. Chemically synthesized oligomers were obtained from the Nucleic Acid Synthesis Facility at Harvard Medical School and 5′-end labeled with [γ-^{32}P]-ATP and polynucleotide kinase (Maxam & Gilbert, 1980; Maniatis et al., 1982). The [5′-^{32}P]d(TTCTCATGT$_9$TTGA) containing 4′ or 5′ deuterium label at T_9, T_{10}, and T_{11} positions was prepared as follows. The primer [5′-^{32}P]d(TTCTCATG) (0.05 mM) was annealed to the template d(TCAAACATGAGAA) (0.06 mM) in 20 mM Tris-HCl (pH 7.5), 10 mM $MgCl_2$, and 0.1 mM dithiothreitol by heating at 90 °C for 2 min followed by slow cooling to room temperature. The dNTPs including 4′ or 5′ ^1H or ^2H labeled TTPs (10- to 13-fold excess) were added to the above reaction mixture, and the chain extension reaction was initiated by 5 units of the Klenow fragment of DNA polymerase. The reaction was allowed to proceed for 45 min at 25 °C, at which time it was terminated by addition of 10 mM EDTA. The [3′-^{32}P]d(TTCTCATGTTTGA) was prepared by a procedure identical with that described above except that [α-^{32}P]dATP was utilized and the primer was not labeled. The labeled oligomers were purified by use of a 20% denaturing polyacrylamide gel.

NCS Reactions. The NCS chromophore was extracted from the native drug as previously described (Kappen & Goldberg, 1985). A standard reaction was carried out in a volume of 25–100 μL containing 20 mM Tris-HCl (pH 8.0), 0.5 mM EDTA, 130 μM [^{32}P]oligomer, NCS, and thiol at concentrations indicated in the figure legends. NCS or thiol was added last to start the reaction.

The reactions carried out under anaerobic conditions followed the procedure previously described by Kappen and Goldberg (1985). The reaction was run in a vessel containing a side arm. The main chamber contained buffer, oligomer, NCS, in concentrations and conditions described above, and 20 mM misonidazole. After removal of the O_2, the reaction was started by the addition of thiol from the side arm. The reaction was allowed to proceed for 30 min at 4 °C.

BLM Reactions. [^{32}P]Oligomers (150 μM) were reacted with premixed bleomycin (5 μM) and ferrous sulfate (15 μM) in 20 mM Tris-HCl (pH 8.0). The reaction was initiated by addition of 10 mM 2-mercaptoethanol and allowed to proceed for 15 min at room temperature.

Alkali and Hydrazine Treatment. Subsequent to drug-mediated cleavage, each solution was made 0.1 M in NaOH and heated at 90 °C for 30 min. The samples were then neutralized with 0.1 N HCl. Alternatively, each solution was made 45 mM in hydrazine hydrochloride (pH 8.0) and incubated for 1 h at room temperature or 90 °C for 5 min.

Analysis of Products via Gel Electrophoresis. The reaction mixture was dried in a Speed-Vac concentrator and the dried pellet dissolved in 80% formamide containing 1 mM EDTA and marker dyes. The samples were electrophoresed on a 20% urea-containing polyacrylamide gel. The gel band intensities were quantitated by scanning an autoradiogram using an LKB Ultroscan laser densitometer or a Molecular Dynamics phosphorimager with Imagequant Version II β-1 for data manipulation. In some experiments the peaks of interest were cut out of the densitometric traces illustrated in Figure 5B and weighed on an analytical balance.

Isolation and Characterization of 3′-Phosphoglycolate Ends. The bands corresponding to 3′-glycolate-ended oligomers produced in the drug reactions using the 7-mer, [^{32}P]d(TGTTTGA), and the 13-mer, [^{32}P]d(TTCTCATGTTTGA), were excised from the gel, crushed, and stirred in 1 M triethylammonium carbonate, pH 7.6, for 6–12 h at room temperature. After the removal of gel slices by centrifugation the supernatant was diluted 5-fold with H_2O. The solution was loaded onto a Sep-Pak cartridge. After washing the column with 25 mM triethylammonium carbonate, the products from the 7-mer and the 13-mer were eluted with H_2O and 50% acetonitrile, respectively. Samples were dried in a Speed-Vac concentrator. The pellets were then dissolved in H_2O for further analysis.

The glycolate product from the 7-mer was analyzed by HPLC on a μBondapak C_{18} column using isocratic elution with 0.1 M ammonium formate, pH 6.0 (retention time 8 min). Thin-layer chromatographic analysis of the same material on silica gel (2-propanol/NH_4OH/H_2O, 7:3:2) gave an R_f of 0.26.

The glycolate product (10^4 cpm) isolated from the 13-mer was annealed to an excess of the complementary strand of the original 13-mer. This product was incubated in 25 mM Tris-HCl (pH 8.0), 120 mM NaCl, 1.3 mM dithiothreitol, and endonuclease IV (0.75 unit) for 24 h at 4 °C. The solvent was then removed from the samples, which were then analyzed on a 20% sequencing gel.

Results and Discussion

Characterization of the 3′-Phosphoglycolate Terminus. Previous studies of Frank et al. (1990) using a 375 bp fragment of pBR322 demonstrated that at certain dGTT sequences, NCS* abstracted a C-4′ hydrogen atom, resulting in the production of putative 3′-phosphoglycolates and, subsequent to piperidine treatment, 3′-phosphate termini (Scheme IB). The former was tentatively identified on the basis of its identical electrophoretic mobility to that of the bleomycin-induced 3′-phosphoglycolate lesion in the same sequence. In order to facilitate a more extensive chemical characterization and quantitation of the products resulting from 4′-chemistry by NCS and to assess the isotope effects on their production, two oligomers d(TGTTTGA) and d(TTCTCATGTTTGA) were used as substrates for the drug. Previous studies of Frank et al. (1990) suggested that acidic thiols afforded the greatest extent of phosphoglycolate production. To establish the conditions required to optimize the production of the putative 3′-phosphoglycolate ends for characterization, the NCS reaction with the heptamer [5′-^{32}P]TGTTTGA was examined as a function of thiol (Figure 1). Two bands are observed at the T_3 residue on a DNA sequencing gel when acidic thiols (lanes 4–6) are used to activate the drug. The slower moving band has the same mobility as that of the 3′-phosphate marker, while the faster moving band (arrow) has a mobility coincident with that of the 3′-glycolate fragment (TG-glycolate) produced by bleomycin (lane 9). Overall cleavage at this T residue is the least of the three consecutive T residues. With neutral thiols (lanes 7 and 8) the amount of TG-glycolate is proportionally much less as determined by densitometry and discussed in detail subsequently.

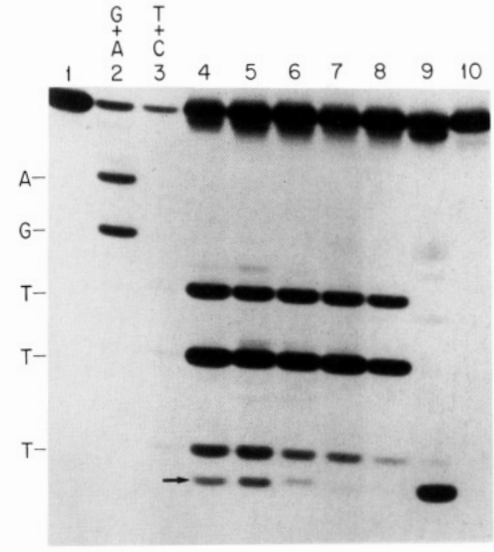

FIGURE 1: Effect of various thiols on NCS-induced strand scission. 5′-^{32}P-Labeled 7-mer, d(TGTTTGA) (131 μM), was treated with NCS chromophore (57 μM) in a standard reaction. The products were analyzed on a sequencing gel. G+A and T+C represent Maxam-Gilbert markers. In lanes 4–8, the oligomer was treated with NCS in the presence of the thiols indicated. Lanes: (4) gluathione; (5) 3-mercaptopropionate; (6) 2-mercaptoethanesulfonate; (7) 2-mercaptoethanol; (8) dithiothreitol. All thiols were at 5 mM except 2-mercaptoethanol (10 mM). Lane 9 contains the oligomer treated with bleomycin as described under Materials and Methods. Lanes 1 and 10 are no drug controls containing 2-mercaptoethanesulfonate and 2-mercaptoethanol, respectively. Arrow indicates 3′-glycolate product.

The TG-glycolates from both NCS and mercaptopropionate treatment and bleomycin treatment were isolated from the sequencing gel and shown to cochromatograph on a reverse-phase HPLC column (retention time 8 min) and on thin-layer chromatography (silica gel, R_f 0.26). Additional characterization of the glycolate fragment indicated that treatment with alkali or the 3′-phosphatase activity associated with T_4 polynucleotide kinase had no effect on its electrophoretic mobility. By contrast, treatment with *E. coli* endonuclease IV (performed on the fragment derived from the NCS-treated 13-mer) resulted in a shift in its electrophoretic mobility to that of a 3′-hydroxyl-ended fragment (data not shown). These results strongly support the identification of the product

corresponding to the faster moving band produced by NCS attack at T as an oligomer possessing a 3′-phosphoglycolate terminus. The direct formation of 3′-glycolate-ended product in addition to a 3′-phosphate-ended fragment suggests that two separate chemical reactions occur at this T residue, one involving 4′-chemistry and the other 5′-chemistry.

Isotope Effects on the Partitioning between 4′- and 5′-Chemistry. Analysis by gel electrophoresis of specifically deuteriated ^{32}P-end-labeled DNA treated with DNA-cleaving drugs has been used to detect and quantitate rate-limiting carbon–hydrogen bond cleavages at individual sequence sites, such as at GPyr sites (C-4′) by bleomycin (Kozarich et al., 1989) and at the minor site d(AGC) (C-1′) by NCS (Kappen et al., 1990). Therefore, an experiment was carried out with the 13-mer, [5′-^{32}P]d(TTCTCATGT$_9$TTGA), in which the 4′-hydrogens of T$_9$, T$_{10}$, and T$_{11}$ were replaced by deuterium. Observation of an isotope effect on the production of the 3′-glycolate fragment would confirm that this product is the result of NCS-mediated 4′-hydrogen atom abstraction. As seen in Figure 2A, with mercaptopropionic acid as the activating thiol, a distinct isotope effect was observed in the formation of the 3′-glycolate-ended fragment at T$_9$ in the 4′-deuteriated substrate (compare lanes 3 and 5). Deuterium substitution for hydrogen at the 5′-positions of the same T residues shows a smaller but definite isotope effect in the formation of the 3′-phosphate-ended fragment at T$_9$ (compare lanes 3 and 4). Further, there is a concomitant increase in the formation of the 3′-glycolate-ended product with the 5′-deuteriated substrate, indicating that the rate of 4′-hydrogen atom abstraction increases at the expense of 5′-deuterium abstraction. Similarly, a slight increase in the 3′-phosphate product is observed with the 4′-deuteriated substrate. Quantitation of the isotope effects by densitometry revealed a k_H/k_D at C-4′ of 4.0 ± 0.6 and at C-5′ of 1.6 ± 0.2 (average of five determinations). It should also be noted that there are no significant isotope effects on the formation of 3′-phosphate-ended fragments resulting from major strand breakage at T$_{10}$ and T$_{11}$, consistent with previous observations in DNA restriction fragments (Frank et al., 1990).

Additional support for a mechanism involving 4′-hydrogen atom abstraction in the formation of the 3′-glycolate fragment is provided by an experiment using [3′-^{32}P]-13-mer (Figure 2B). With the 4′-deuteriated oligomer an isotope effect of 3.9, comparable to that described before, was found in the formation of a 5′-phosphate-ended fragment (compare lanes 4 and 8 at T$_9$). This is the expected product at the 3′-end of the break resulting from 4′-chemistry. Alkali treatment of the [3′-^{32}P]oligomer resulted in elmination of the thymidine 5′-aldehyde moiety, the product of 5′-chemistry, affording a 5′-phosphate. The intensities of the bands at the three T residues T$_9$, T$_{10}$, and T$_{11}$ were enhanced, especially T$_{10}$ and T$_{11}$ (see lanes 5, 7, and 9). In separate experiments (data not shown), the band containing the putative nucleoside 5′-aldehyde (observed at the top of the gel in lanes 4, 6, and 8) was isolated from the gel and treated with alkali to produce the expected 5′-phosphate fragments. In addition, alkali-labile breaks were associated with the 4′-hydroxylation (Scheme IB).

The intensity of the bands after alkali treatment, corresponding in mobility to the 5′-phosphate markers, is a measure of the total reaction (direct cleavage plus alkali-labile components) at these sites. On an underexposed film the band from the 4′-deuteriated oligomer at T$_9$ was found to be significantly less (50%, average of 3 experiments) (Figure 2B, lane 9) than that from the protio-containing (lane 5) or the 5′-deuteriated oligomers (lane 7). In contrast to these results

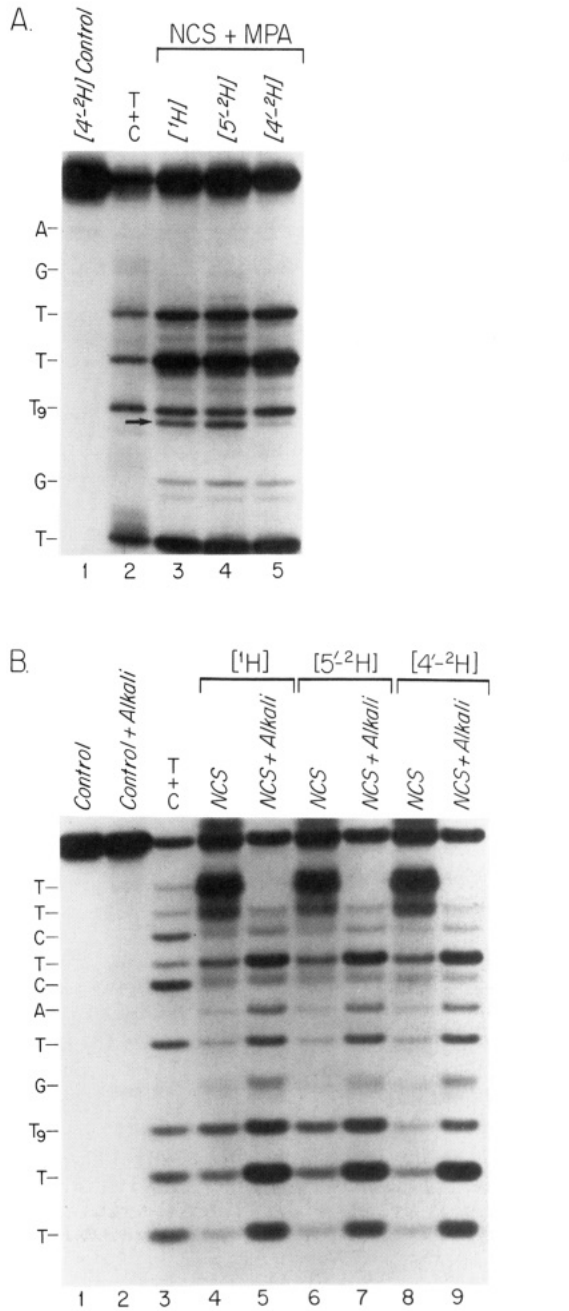

FIGURE 2: Effect of deuterium labeling on NCS-induced cleavage of 5′- and 3′-end-labeled oligonucleotides. (A) [5′-^{32}P]d(TTCTCATGTTTGA) (126 μM) annealed to its complementary 13-mer was treated with 57 μM NCS in the presence of 5 mM 3-mercaptopropionate (MPA) under standard conditions. The reaction mixture was analyzed on a sequencing gel. Lane 2 represents T+C Maxam-Gilbert marker. Arrow indicates the 3′-glycolate-ended fragment. (B) Reaction conditions are the same as in Figure 2A except that d(TTCTCATGTTTG^{32}pA) was the substrate for NCS in the presence of 5 mM 3-mercaptopropionate. Alkali treatment was as under Materials and Methods.

deuterium labeling at 4′- or 5′-positions did not significantly affect the total damage at T$_{10}$ or T$_{11}$ (compare lanes 5, 7, and 9). Substantially less total damage at T$_9$ with 4′-^{2}H labeling in comparison with 5′-^{2}H labeling suggests that damage may result from alternative binding modes of NCS in this region. If in fact the same mode of NCS binding resulted in cleavage at both the 4′- and 5′-positions, then the total damage at T$_9$ might have been expected to be independent of the isotopic substitution.

Results with 5′- and 3′-labeled oligomers clearly demonstrate partitioning between 4′- and 5′-chemistry uniquely at T$_9$ in

Table I: Effect of Deuterium Substitution on Alkali-Dependent Cleavage at T_9[a]

isotope at T_9	area under PO_4 band at T_9		% increase due to alkali
	−alkali	+alkali	
^1H	1.01	1.56	54
5′-^2H	0.61	1.50	146
4′-^2H	0.89	1.04	17

[a] The intensity of the band of the 3′-phosphate-ended cleavage fragment at T_9 in Figure 3 was quantitated by densitometry of a lightly exposed X-ray film.

these oligomers. The mode or modes of NCS binding required to effect strand scission require further investigation. In fact, recent studies, compatible with different binding modes, have shown that double-strand breaks at the T residues in d(AGT)·d(ACT) sequences are due to predominantly 4′-chemistry at the d(GT) step and 5′-chemistry at the d(CT) step, whereas single-stranded breaks at each involve mainly 5′-chemistry (Dedon & Goldberg, 1990). The importance of subtleties of sequence is emphasized by the finding that when dI, which simply lacks a 2-amino group in the minor groove of DNA, is substituted for dG at a d(GT) step in the 13-mer, no 3′-phosphoglycolate is observed (data not shown). Furthermore, the 5′-labeling experiments demonstrate yet another example of sequence-selective isotope effects.

Effect of Deuterium Substitution on Alkali-Dependent Cleavage at T_9. As discussed above, the 4′-hydroxylated abasic product, first identified by Saito et al. (1989), leads to a strand break with 3′-phosphate-ended termini upon alkali treatment. Therefore, the alkali-induced increase in 3′-phosphoryl ends is a measure of 4′-hydroxylation. In order to determine the extent of C-4′ hydroxylation in the reaction involving 4′-hydrogen abstraction, the NCS reaction products from the [5′-^{32}P]-13-mer were treated with alkali and the increase in the intensity of the band corresponding to the fragment with a 3′-phosphate was measured for the different isotopically labeled substrates (Figure 3, Table I). In a typical experiment the intensity at the 3′-phosphate region increased upon alkali treatment; this was most striking with the 5′-$^2H_2$-labeled substrate and least with the 4′-^2H-labeled substrate (compare lanes 4, 6, and 8 at T_9), consistent with a 4′-isotope selection effect on the formation of the alkali-labile 4′-hydroxylation product that then eliminates the sugar moiety on alkali treatment. This result was further supported by an experiment involving conversion of the putative 4′-hydroxylation product (**8**) (Scheme IB) to its pyridazine derivative (Sugiyama et al., 1988, 1990). As shown in Figure 4, there is a faint band (arrow a) with a slightly faster mobility than the 3′-phosphate band at T_{10}. This band disappears upon alkali treatment (Figure 3) and is probably produced by phosphate elimination at the 3′-side of the damaged sugar residue at T_9 (**10**, Scheme IB) (Frank et al., 1990). Since formation of **10** is variable and dependent on workup conditions (Frank et al., 1990), a more quantitative measure of **8** was sought involving its conversion to a stable reaction product associated with a strand break so that it could be identified on a sequencing gel. When the NCS reaction is directly treated with hydrazine (Figure 4), a new band (arrow b) appears with a slightly faster mobility than the one designated by arrow a (compare lanes 1 and 2), presumably the pyridazine derivative.

As expected, treatment of a bleomycin reaction with hydrazine produces the same band (lane 6). The reaction of **8** with hydrazine was quantitative and equivalent to the increase in 3′-phosphate ends under alkaline conditions (unpublished results) observed with the bleomycin reaction (lane 6) (Rabow et al., 1990a,b). Band b exhibits a substantial 4′-deuterium isotope effect (lanes 2 and 4). Densitometric measurements of the alkali-dependent increase at the 3′-phosphate at T_9 (Figure 3) and the pyridazine derivative at T_9 give an isotope effect of 3.7 with the 4′-deuteriated substrate, a value in close agreement to that obtained for the 3′-glycolate at T_9. These data are consistent with the presence of a common intermediate in the formation of the C-4′ lesions.

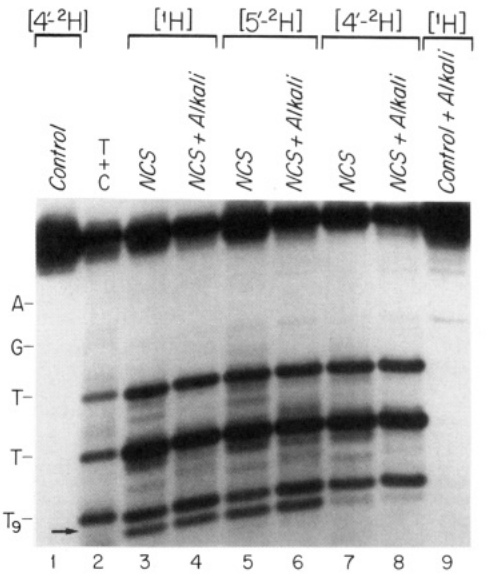

FIGURE 3: Alkali-stimulated cleavage of selectively deuteriated oligonucleotide by NCS. [5′-^{32}P]d(TTCTCATGTTTGA) was the substrate for NCS in the presence of 5 mM 3-mercaptopropionate in a reaction identical with that in Figure 2A. Arrow indicates the 3′-glycolate-ended fragment. Lanes 4, 6, and 8 represent alkali-treated drug reactions.

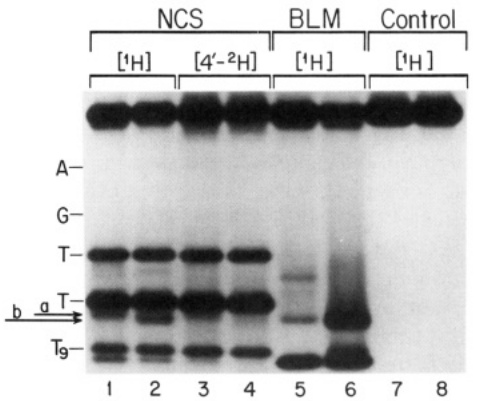

FIGURE 4: 4′-Deuterium isotope selection effect on the formation of the pyridazine derivative of the 4′-hydroxylated product generated by NCS. A standard reaction contained [5′-^{32}P]d(TTCTCATGTTTGA) (171 μM), NCS (53 μM), and 5 mM 3-mercaptopropionate. Portions of the reaction mixture were treated with hydrazine (lanes 2, 4, and 6) prior to gel electrophoresis. Lanes 5 and 6, bleomycin (BLM) treatment.

Effects of Thiol Structure on the Partitioning between 4′- and 5′-Chemistry and on the C4′ Partitioning between 3′-Phosphoglycolate and Alkali-Labile 3′-Phosphate Ends. The first step in activation of NCS involves a nucleophilic 1,4-addition of a thiol at C-12 (Scheme II). Since the size, shape, and charge of the activated drug (NCS*) will differ depending upon the thiol, these differences might result in changes in binding to the minor groove of the DNA as well as the orientation of NCS* for attack on the deoxyribose moiety of DNA. The thiol has also been proposed to play additional roles in the drug-mediated DNA cleavage: reduction of the putative 4′-peroxy radical **5** to produce the 4′-hydroperoxide **6**, as well

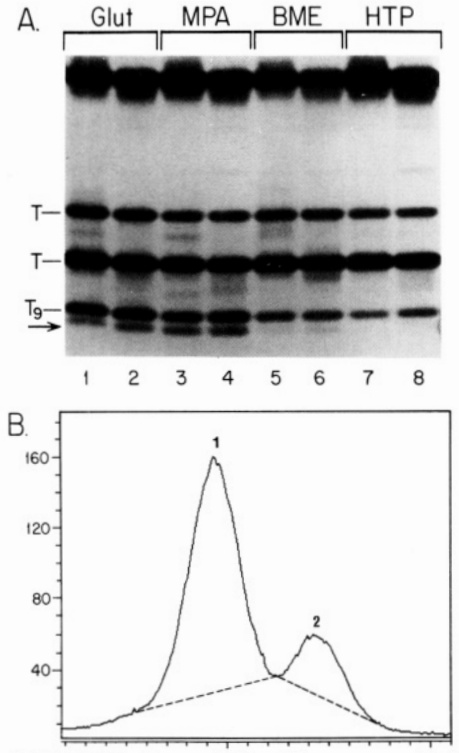

FIGURE 5: (A) [5′-^{32}P]-13-mer (171 μM) was treated with 42 μM NCS chromophore in the presence of 5 mM thiol (glu, MPA, or HTP) or 10 mM BME under standard conditions (lanes 1, 3, 5, and 7). Alkali conditions were as described under Materials and Methods (lanes 2, 4, 6, and 8). (B) Densitometry tracing of the T_9 region of the gel in Figure 5A, lane 4, using a Molecular Dynamics phosphorimager. Peak 1 corresponds to the 3′-phosphate region, and peak 2 corresponds to the 3′-phosphoglycolate region. The relative amounts of T_9-3′-phosphate and T_9-3′-phosphoglycolate ends were determined by cutting and weighing each peak above the dashed line.

as reduction of the hydroperoxide to effect partitioning at C-4′ between phosphoglycolate ends (**9**) and alkali-labile 3′-phosphate ends (**8**, Scheme IB). The findings reported in Figure 1 clearly indicate that acidic thiols favor production of 3′-glycolate ends over neutral thiols. In addition, previous studies of Saito et al. (1989) with neutral hydroxythiophenol reported only production of **8** (Scheme IB).[2]

An experiment was designed, therefore, to examine the effect of thiols on the partitioning between C-4′ and C-5′ chemistry and on the C-4′ partitioning. The [5′-^{32}P]-13-mer was incubated with NCS and one of four thiols (mercaptopropionic acid, glutathione, 2-mercaptoethanol, and hydroxythiophenol). Results of the analysis of the products by gel electrophoresis under neutral and alkaline conditions are shown in Figure 5A. The total damage of T_9 due to C-5′ and C-4′ chemistry can be assessed by determining the total amount of radioactivity in the 3′-phosphate-ended fragment and the 3′-glycolate-ended fragment (arrow) (Figure 5A) under alkaline conditions. As indicated in Table II, acidic thiols are much more efficient at total cleavage than neutral thiols by a factor of approximately 2 or 3:1. The ratio of C-4′ to C-5′ chemistry can be determined as follows. Non-alkali-dependent cleavage represents C-5′ chemistry as a 3′-phosphate end and C-4′ chemistry as a phosphoglycolate end (lanes 1, 3, 5, and 7, Figure 5A). The partitioning between the two can be established by densitometry (Figure 5B). In addition, one needs to consider the cleavage at 4′ (Scheme IB) that is only observable subsequent to alkaline treatment. Assuming alkaline treatment does not affect the amount of 3′-phosphoglycolate produced, the amount of alkali-labile 3′-phosphate due to 4′ cleavage can be assessed by subtracting the total amounts of radioactivity at T_9, lanes 1, 3, 5, and 7 (non alkali treated), from the corresponding radioactivity at T_9 in lanes 2, 4, 6, and 8 (alkali treated). The ratio of 4′/5′ cleavage therefore can be calculated as a function of thiol and is also indicated in Table II.

[2] Saito et al. (1989) reported less than 3% glycolate. Whether this is their lower limit of detection or they actually observed some glycolate ends is unclear.

Table II: Effect of Thiols on C-4′, C-5′, and C-4′ Partitioning

thiol	total cleavage[a] (%)	4′/5′ cleavage	total cleavage of 4′ (%)	% glycolate
MPA	98	0.73	42	38
Glu	100	0.46	31	29
BME	42	0.29	22	18
HTP	30	0.44	27	6[b]

[a] Glu-dependent cleavage was taken as 100%. [b] Overestimate of the amount of glycolate due to background.

Scheme III

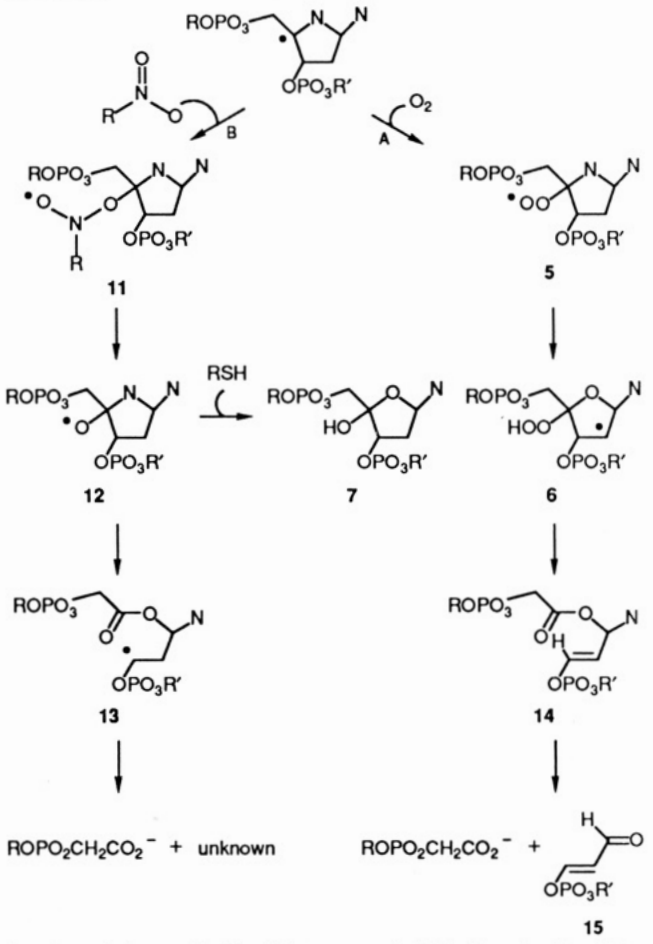

From these data we can also establish the partitioning at C-4′ between 3′-phosphoglycolate and 3′-phosphate (Table II). The results indicate that, compared to charged thiols, neutral thiols give less cleavage overall at T_9. No general trend however is apparent that would allow a distinction to be made between the behavior of neutral and acidic thiols, when examining the ratio of 4′ to 5′ cleavage or the total observed 4′ cleavage at T_9. On the basis of recent studies of Sugiyama et al. (1990) on calf thymus DNA that suggest that 17% of the cleavage occurs at the C-4′ positions of deoxyribose, these thiols must be examined, with additional sequences, to see if any interesting trends become apparent. It is clear that unraveling these effects will also require a dissection of the bimodal function of thiol as an activator/reductant. This could

be achieved by using an alternative method of activation of NCS, such as with a strong nucleophilic species which cannot function as a reductant.

Evidence for 4′-Radical Intermediates: Trapping with O_2 and Misonidazole. The studies described above clearly demonstrate that NCS* can effect novel chemistry at C-4′. The question then arises as to what possible mechanisms can account for the observed results. Formation of the products resulting from C-5′ and C-1′ chemistry induced by NCS has previously been shown to be dependent upon trapping of the putative radical intermediates by O_2 (Kappen & Goldberg, 1984; Kappen et al., 1988). Furthermore, isotopic labeling studies with the nitroaromatic radiosensitizer misonidazole have indicated that it can be also function efficiently to trap the same putative deoxyribose radical generated by NCS* (Chin et al., 1987; Kappen et al., 1989). Misondiazole in those cases has been shown to efficiently substitute for O_2 in effecting strand scission. Both O_2 and misonidazole are presumably acting as effective radical scavengers. Therefore, it was of interest to establish the effect of O_2 depletion on the products resulting from 4′-chemistry, that is, whether a 4′-radical might be involved as indicated in Scheme IB. Furthermore, recent studies of Rabow et al. (1990b) have shown that in Fe·BLM-mediated production of **8** (Scheme IB) the oxygen of the hydroxyl group is derived from solvent and not O_2. As shown in Figure 6A, depletion of O_2 results in marked reduction, at all residues, of NCS-induced DNA strand cleavage including that due to 4′-chemistry at T_9 (compare lanes 3 and 4 with 5 and 6). In contrast to bleomycin, therefore, these results indicate that 4′-hydroxylated product **8** is the result ultimately of trapping of a C-4′ radical by O_2. Bands migrating slower than the starting material in the anaerobic reactions (within brackets, lanes 3 and 4) presumably represent covalent adducts between NCS and DNA deoxyribose, similar to those reported by Povirk and Goldberg (1985b). Addition of misonidazole to the anaerobic reaction mixture dramatically restores all DNA cleavage products at T9: both glycolate and **8** (lanes 1 and 2). In fact, the glycolate band is somewhat stronger than that in the aerobic reaction (lanes 5 and 6). The amount of the 4′-hydroxylation product relative to the 3′-glycolate-ended fragment appears to be less under anaerobiosis with misonidazole than under aerobiosis. As expected, both 4′-cleavage products, the 3′-glycolate (compare lanes 1 and 4 in Figure 6B) and the 4′-hydroxylation product, show comparable 4′-isotope selection effects (Figure 6B) as measured by the alkali-dependent increase in 3′-phosphate ends or by derivatization to its pyridazine derivative (arrow, Figure 6B, lanes 3 and 6). Thus, both O_2 and misonidazole appear to effectively trap the putative 4′-radical intermediate.

An even more intriguing observation is that the damaged sugar products that have been characterized thus far for NCS-mediated C-4′ chemistry are identical with those characterized for bleomycin-mediated DNA degradation (Stubbe & Kozarich, 1987). The fate or fates of the three-carbon sugar fragment accompanying production of 3′-phosphoglycolate ends, however, remain to be established. The low levels of C-4′ chemistry relative to C-5′ chemistry make this task analtyically challenging. Unlike bleomycin, however, O_2 is required to produce *both* C-4′ derived products. Understanding the mechanism of phosphoglycolate production in the case of NCS with both O_2 and misonidazole may shed some light on the elusive mechanism by which the same product is produced by bleomycin.

The following model may be put forth to accommodate results thus far available (Scheme III). In one case, Scheme

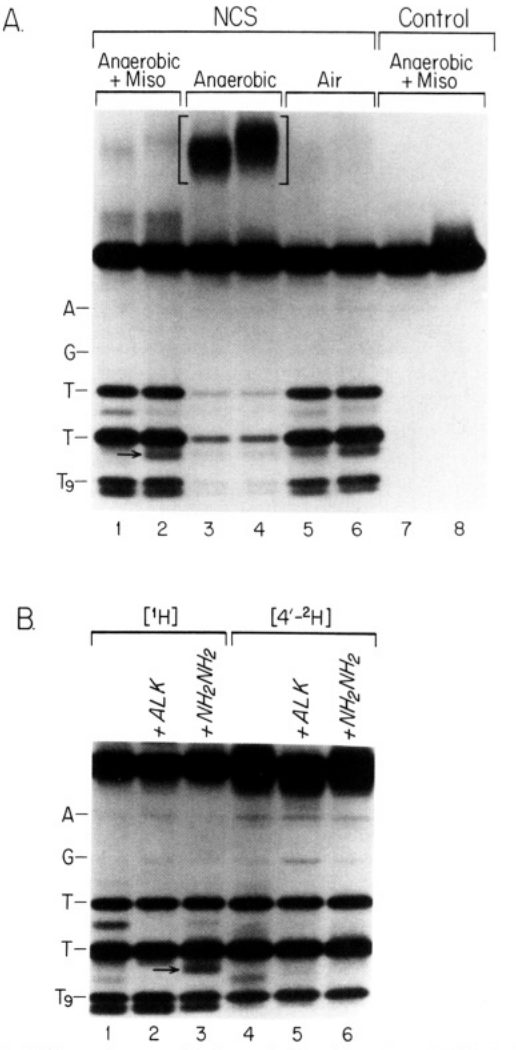

FIGURE 6: Effect of anaerobiosis and misonidazole on NCS-induced strand breakage. (A) 5′-^{32}P-End-labeled 13-mer (130 μM) was the substrate for NCS (55 μM) in the standard reaction performed under anaerobic/air conditions with or without misonidazole as described under Materials and Methods. In lanes 2, 4, 6, and 8, the reaction mixtures were treated with hydrazine prior to gel analysis. (B) Effect of deuterium substitution at C-4′ in the misonidazole-induced restoration of DNA damage under anaerobiosis. Reaction conditions were the same as in (A), except that the 5′-^{32}P-end-labeled 13-mer had deuterium label at the C-4′ position (lanes 4–6). All samples contained NCS. Arrow indicates the pyridazine derivative of the 4′-hydroxylation product.

IIIA, the 4′-radical is trapped by O_2, and in Scheme IIIB, the radical is trapped by misonidazole. In Scheme IIIB, based on studies of Steenken and Jagannadham (1985), Chin et al. (1987), and Kappen et al. (1989), one can propose that the nitroxyradical adduct (**11**) will be cleaved to produce the 4′-oxy radical **12**. If the 4′-oxygen radical is reduced by thiol, then **8** (Scheme IB), previously characterized by Saito et al. (1989), is formed. However, if this 4′-oxygen radical can undergo a β-scission reaction to produce the 3′-radical **13**, then ultimately a 3′-phosphoglycolate end would result. The fate of the three-carbon fragment depends on the radical trap in solution and is not so easy to predict.

In the case shown in Scheme IIIA, if O_2 traps the putative 4′-radical, then peroxy radical **5** would be produced. While simple peroxy radicals can dimerize to form tetroxides that can undergo a Russell fragmentation to lose O_2 (von Sonntag, 1987; Howard, 1973) and produce alkoxy radicals such as **12**, steric constraints in the case of the oligomers make this scenario unlikely. Alternatively, as shown in Scheme IIIA,

the peroxy radical **5** might abstract the 2′-*pro-R* hydrogen to produce a 2′-radical that undergoes β-fragmentation followed by homolytic cleavage of the peroxide bond to form **14** and HO•.

Production of a 3′-phosphoglycolate end would result in a 5′-modified end that might be expected to have altered electrophoretic mobility. No such modified end is apparent (Figure 2B). The stability of such an adduct to electrophoresis conditions is, however, an unknown. Previous studies of Ajmera et al. (1986b) using [3′-^{18}O]nucleotides have shown for the bleomycin-catalyzed production of phosphoglycolate that similar chemistry cannot occur. Neither the β-fragmentation reaction shown in Scheme IIIB nor that in Scheme IIIA results in the production of stable radicals. The relative rates of fragmentation relative to reduction are hard to predict, with the latter reaction obviously dependent on the structure of the thiol. The mechanistic hypothesis in Scheme III accommodates the known experimental results. Model studies are however required to investigate some of the concerns outlined above and assess the validity of this working hypothesis.

Summary. The results described in this paper establish that NCS* can abstract a 4′-hydrogen atom from the T in the d(GTTT) sequence in an oligonucleotide and that, as in the case of previously characterized 1′-chemistry, a substantial isotope effect exists on this reaction. A smaller, but definitive isotope effect also occurs upon 5′-hydrogen atom abstraction at this same T. However, at the two adjacent Ts (T_{10}, T_{11}) which are substantially more prone to cleavage, *no* apparent isotope effect occurs. The observation of sequence-dependent isotope effects has previously been reported for C-1′ chemistry with NCS and C-4′ chemistry with BLM. Furthermore, substitution of deuterium for hydrogen at C-4′ or C-5′ positions of T_9 causes a shift in the attack rate at each position. Molecular modeling studies reveal that the radical center at C-6 of NCS in the minor groove of DNA is almost equidistant between the 5′- and 4′-hydrogen (Galat & Goldberg, 1990). Whether cleavage at C-4′ and C-5′ is effected by drug bound in the same conformation within the minor groove, however, remains to be established. The structure (shape and charge) of thiols appears to affect binding of drug and partitioning between C-4′ and C-5′ chemistry, as well as intramolecular partitioning at C-4′. A nonreducing nucleophile is required to mediate NCS activation so that the role of the thiols can be addressed. Unexpectedly, the identified products of NCS-mediated C-4′ chemistry are identical with those observed with BLM. The production of phosphoglycolate ends by O_2 and misonidazole trapping without the assistance of a metal-catalyzed Criegee arrangement has important mechanistic implications which require further study.

Acknowledgments

We gratefully acknowledge the help of M. Absalon in the use of the phosphorimager.

References

Ajmera, S., Massof, S., & Kozarich, J. W. (1986a) *J. Labelled Compd. Radiopharm. 23*, 963–968.

Ajmera, S., Wu, J. C., Worth, L., Rabow, L. E., Stubbe, J., & Kozarich, J. W. (1986b) *Biochemistry 25*, 6586.

Brown, H. C., & Subba Rao, B. C. (1960) *J. Am. Chem. Soc. 82*, 681–686.

Chin, D.-H., Kappen, L. S., & Goldberg, I. H. (1987) *Proc. Natl. Acad. Sci. U.S.A. 84*, 7070–7074.

Chin, D.-H., Zeng, C., Costello, C. E., & Goldberg, I. H. (1988) *Biochemistry 27*, 8106–8114.

Dedon, P. C., & Goldberg, I. H. (1990) *J. Biol. Chem. 265*, 14713–14716.

Edo, K., Mizugaki, M., Koide, Y., Seto, H., Furihata, K., Otake, N., & Ishida, N. (1985) *Tetrahedron Lett. 26*, 331–334.

Frank, B. L., Worth, L., Jr., Christner, D. F., Kozarich, J. W., Stubbe, J., Kappen, L. S., & Goldberg, I. H. (1990) *J. Am. Chem. Soc.* (in press).

Galat, A., & Goldberg, I. H. (1990) *Nucleic Acids Res. 18*, 2093–2099.

Goldberg, I. H. (1987) *Free Radical Biol. Med. 3*, 41–54.

Hensens, O. D., Dewey, R. S., Liesch, T. M., Napier, M. A., Reamer, R. A., Smith, J. L., Albers-Schonberg, G., & Goldberg, I. H. (1983) *Biochem. Biophys. Res. Commun. 113*, 538–547.

Howard, J. A. (1973) in *Free Radicals* (Kochi, J. K., Ed.) Vol. 2, pp 3–62, Wiley, New York.

Kappen, L. S., & Goldberg I. H. (1983) *Biochemistry 22*, 4872–4878.

Kappen, L. S., & Goldberg, I. H. (1984) *Proc. Natl. Acad. Sci. U.S.A. 81*, 3312–3316.

Kappen, L. S., & Goldberg, I. H. (1985) *Nucleic Acids Res. 13*, 1637–1648.

Kappen, L. S., & Goldberg, I. H. (1989) *Biochemistry 28*, 1027–1032.

Kappen, L. S., Goldberg, I. H., & Liesch, J. M. (1982) *Proc. Natl. Acad. Sci. U.S.A. 79*, 744–748.

Kappen, L. S., Chen, C., & Goldberg, I. H. (1988) *Biochemistry 27*, 4331–4340.

Kappen, L. S., Lee, T. R., Yang, C., & Goldberg, I. H. (1989) *Biochemistry 28*, 4540–4542.

Kappen, L. S., Goldberg, I. H., Wu, S. H., Stubbe, J., Worth, L., & Kozarich, J. W. (1990) *J. Am. Chem. Soc. 112*, 2797–2798.

Kozarich, J. W., Worth, L., Frank, B. L., Christner, D. F., Vanderwall, D. E., & Stubbe, J. (1989) *Science 245*, 1396–1399.

Maniatis, T., Fritsch, E. F., & Sambrook, J. (1982) in *Molecular Cloning*, Cold Spring Harbor Laboratory, Cold Spring Harbor, New York.

Maxam, A. M., & Gilbert, W. A. (1980) *Methods Enzymol. 65*, 499–560.

Moss, G. P., Reese, C. B., Schofield, K., Shapiro, R., & Todd, L. (1963) *J. Chem. Soc.*, 1149–1154.

Myers, A. G. (1987) *Tetrahedron Lett. 28*, 4493–4496.

Myers, A. G., Proteau, P. J., & Handel, T. M. (1988) *J. Am. Chem. Soc. 110*, 7212–7214.

Povirk, L. F., & Goldberg, I. H. (1985a) *Proc. Natl. Acad. Sci. U.S.A. 82*, 3182–3186.

Povirk, L. F., & Goldberg, I. H. (1985b) *Biochemistry 24*, 4035–4040.

Povirk, L. F., & Goldberg, I. H. (1986) *Nucleic Acids Res. 14*, 1417–1426.

Rabow, L. E., Stubbe, J., & Kozarich, J. W. (1990a) *J. Am. Chem. Soc. 112*, 3196–3203.

Rabow, L. E., McGall, G., Stubbe, J., & Kozarich, J. W. (1990b) *J. Am. Chem. Soc. 112*, 3203–3208.

Saito, I., Kawabata, H., Fujiwara, T., Sugiyama, H., & Matsuura, T. (1989) *J. Am. Chem. Soc. 111*, 8302–8303.

Steenken, S., & Jagannadham, V. (1985) *J. Am. Chem. Soc. 107*, 6818–6826.

Stubbe, J., & Kozarich, J. W. (1987) *Chem. Rev. 87*, 1107–1136.

Sugiyama, H., Xu, C., Murugesan, N., Hecht, S. M., van der

Marel, G. A., & van Boom, J. H. (1988) *Biochemistry 27*, 58-67.
Sugiyama, H., Kawabata, H., Fujiwara, T., Dannoue, Y., & Saito, I. A. (1990) *J. Am. Chem. Soc. 112*, 5252-5257.
von Sonntag, C. (1987) in *The Chemical Basis of Radiation Biology*, Taylor & Francis, London.
Wu, J. C., Kozarich, J. W., & Stubbe, J. (1983) *J. Biol. Chem. 258*, 4694-4697.

Alternative Secondary Structures in the 5′ Exon Affect both Forward and Reverse Self-Splicing of the *Tetrahymena* Intervening Sequence RNA†

Sarah A. Woodson‡ and Thomas R. Cech*
Department of Chemistry and Biochemistry, Howard Hughes Medical Institute, University of Colorado, Boulder, Colorado 80309-0215

Received September 19, 1990; Revised Manuscript Received November 26, 1990

ABSTRACT: The natural splice junction of the *Tetrahymena* large ribosomal RNA is flanked by hairpins that are phylogenetically conserved. The stem immediately preceding the splice junction involves nucleotides that also base pair with the internal guide sequence of the intervening sequence during splicing. Thus, precursors which contain wild-type exons can form two alternative helices. We have constructed a series of RNAs where the stem-loop in the 5′ exon is more or less stable than in the wild-type precursor, and tested them in both forward and reverse self-splicing reactions. The presence of a stable hairpin in ligated exon substrates interferes with the ability of the intervening sequence to integrate at the splice junction. Similarly, the presence of the wild-type hairpin in the 5′ exon reduces the rate of splicing 20-fold in short precursors. The data are consistent with a competition between unproductive formation of a hairpin in the 5′ exon and productive pairing of the 5′ exon with the internal guide sequence. The reduction of splicing by a hairpin that is a normal feature of rRNA structure is surprising; we propose that this attenuation is relieved in the natural splicing environment.

Efficient and accurate RNA splicing requires that the correct splice sites are recognized by the splicing machinery and that other sites are discriminated against. In nuclear mRNA splicing, there is evidence that exon sequences can affect splice site choice (Reed & Maniatis, 1986; Somasekhar & Mertz, 1985). Since splicing of mRNAs is carried out by a complex assembly of small nuclear RNAs and protein factors, it is difficult to sort out which interaction is altered by changes in exon sequence. In self-splicing of the *Tetrahymena* intervening sequence (IVS)[1] or intron, excision of the intron and ligation of the exons is catalyzed by the intron RNA itself (Kruger et al., 1982). In this comparatively simple RNA-only system, we can understand some of the effects of exon sequences in self-splicing on a molecular level.

The *Tetrahymena* IVS is a member of a class of introns, called group I, which share a common secondary structure and mechanism of splicing [reviewed in Cech (1990)]. The mechanism of self-splicing is outlined in Figure 1. The complete reaction consists of two phosphodiester transesterifications. In the first step, the 5′ splice site is cleaved by addition of an exogenous GTP to the 5′ end of the IVS. In the second step, the 3′ splice site is cleaved, resulting in ligation of the exons and release of linear IVS RNA. In addition to the properly folded intron, the reaction depends only on magnesium ion and guanosine or GTP concentration. Base-pairing between nucleotides in the 5′ exon and a polypurine sequence in the IVS called the internal guide sequence (IGS) is conserved among group I introns (Davies et al., 1982; Michel et al., 1982). This pairing, designated "P1" (Burke et al., 1987), enables recognition of the 5′ splice site and is required for self-splicing (Been & Cech, 1986; Waring et al., 1986). Another pairing, "P10," which joins an adjacent portion of the IGS with nucleotides in the 3′ exon (Davies et al., 1982), aids in 3′ splice site recognition (Michel et al., 1989; Suh & Waring, 1990), although it is neither necessary nor sufficient for that process (Price & Cech, 1988).

We have previously shown that splicing of the *Tetrahymena* IVS is fully reversible (Woodson & Cech, 1989). The reverse splicing reaction follows the same pathway as the forward reaction outlined in Figure 1, but in the opposite direction. The products of the forward reaction, linear IVS and ligated exons, are now the reactants. Integration of the IVS back into the splice junction of the exons produces a molecule which contains the splice site sequences of the precursor. Reverse splicing is promoted by high magnesium ion and RNA concentration, and the absence of GTP. As in the case of the forward reaction, recognition of the substrate by the IVS RNA depends on base-pairing between nucleotides immediately upstream of the splice junction and the IGS. Natural 3′ exon sequences are not essential for intron integration.

The natural splice junction of the *Tetrahymena* IVS is immediately flanked by two stem-loops that are phylogenetically conserved in the mature rRNA (Clark et al., 1984;

† S.A.W. was supported by a postdoctoral fellowship from the American Cancer Society. T.R.C. is an investigator of the Howard Hughes Medical Institute and American Cancer Society Professor.
* Author to whom correspondence should be addressed.
‡ Present address: Department of Chemistry and Biochemistry, University of Maryland, College Park, MD 20742.

[1] Abbreviations: CHES, 2-(*N*-cyclohexylamino)ethanesulfonic acid; EDTA, ethylenediaminetetraacetic acid; HEPES, *N*-(2-hydroxyethyl)-piperazine-*N*′-2-ethanesulfonic acid; IVS, intervening sequence or intron; IGS, internal guide sequence; LE, ligated exon(s); RNase P, ribonuclease P; rRNA, ribosomal ribonucleic acid; Tris, tris(hydroxymethyl)aminomethane; wt, wild type.

0006-2960/91/0430-2042$02.50/0